MRS. TRACY ADOLE (Orcid ID : 0000-0002-9730-4152)

Article type : Primary Research Articles

Title

Large scale pre-rain vegetation green up across Africa

Running head

Pre-rain vegetation green up

Tracy Adole[1], T.Adole@soton.ac.uk

Jadunandan Dash[1], J.DASH@soton.ac.uk

Peter M. Atkinson[2, 1, 3,] pma@lancaster.ac.uk

[1]Global Environmental Change and Earth Observation Research Group, Geography and Environment, University of Southampton, Southampton SO17 1BJ, UK.

[2]Faculty of Science and Technology, Lancaster University, Lancaster LA1 4YR, UK.

[3]School of Geography, Archaeology and Palaeoecology, Queen's University Belfast, Belfast BT7 1NN, Northern Ireland, UK.

[4]Chinese Academy of Sciences, Beijing, 11A Datun Road, Beijing, China.

Corresponding author: Tracy Adole, T.Adole@soton.ac.uk, Global Environmental Change and Earth Observation Research Group, Geography and Environment, University of Southampton.

Type of paper: Primary Research Article

Keywords: Vegetation phenology; Africa; ecosystem models; climate change; rainfall

Abstract

Information on the response of vegetation to different environmental drivers, including rainfall, forms a critical input to ecosystem models. Currently, such models are run based on parameters that, in some cases, are either assumed or lack supporting evidence (e.g., that vegetation growth across Africa is rainfall-driven). A limited number of studies have reported that the onset of rain across Africa does not fully explain the onset of vegetation growth, for example, drawing on the observation of pre-rain flush effects in some parts of Africa. The spatial extent of this pre-rain green-up effect, however, remains unknown, leaving a large gap in our understanding that may bias ecosystem modelling. This paper provides the most comprehensive spatial assessment to-date of the magnitude and frequency of the different patterns of phenology response to rainfall across Africa, and for different vegetation types. To define the relations between phenology and rainfall, we investigated the spatial variation in the difference, in number of days, between the start of rainy season (SRS) and start of vegetation growing season (SOS); and between the end of rainy season (ERS) and end of vegetation growing season (EOS). We reveal a much more extensive spread of pre-rain green-up over Africa than previously reported, with pre-rain green-up being the norm rather than the exception. We also show the relative sparsity of post-rain green-up, confined largely to the Sudano-Sahel region. While the pre-rain green-up phenomenon is well documented, its large spatial extent was not anticipated. Our results, thus, contrast with the widely held view that rainfall drives the onset and end of the vegetation growing season across Africa. Our findings point to a much more nuanced role of rainfall in Africa's vegetation growth cycle than previously thought, specifically as one of a set of several drivers, with important implications for ecosystem modelling.

Introduction

The African continent contains the world's largest area of savanna and around 17% of the world's tropical forests. Savannas alone account for 30% of the primary production from global terrestrial vegetation, underlining the importance of the African vegetation (Grace *et al.*, 2006). Indeed, African vegetation contributes 38% of the global climate-carbon cycle feedback (Friedlingstein *et al.*, 2010). In spite of this, African vegetation is relatively under-studied (Adole *et al.*, 2016), and the few existing vegetation models are associated with significant uncertainties (Scheiter & Higgins, 2009; Hemming *et al.*, 2013). Another fundamental concern is the vulnerability of African vegetation to climate change, further worsened by interactions between changes in climatic drivers and anthropogenic land use, which puts at risk both the condition and the amount of overall vegetation cover (IPCC, 2014). Apart from their role in global carbon sequestration, the savannas and forests of Africa support a large number of ecosystem services, which are also vulnerable to climatic and anthropogenic changes; for example, the perceived threat to livestock farming and production due to expanding woodlands (Skowno *et al.*, 2016), and reduced crop productivity caused by increasing temperatures and changes in precipitation (Brown & Funk, 2008). These ecosystem services, in addition to their functions, are influenced heavily by the condition of vegetation and its seasonality (Brottem *et al.*, 2014), which could lead to multiple feedbacks into the climate system (Keenan *et al.*, 2014; Buitenwerf *et al.*, 2015; Wu *et al.*, 2016). In the context of anthropogenic, agro-climatic and climate changes, which may affect future ecosystem services, greater understanding of vegetation dynamics across Africa and its drivers is crucial.

In recent years, the importance of phenology has increased as a result of a wide range of empirical-, modelling- and meta-analysis-based evidence, suggesting that long-term changes in key phenological parameters such as the start of season and end of season are key indicators of biological impact resulting from climate change (Cleland *et al.*, 2007; Richardson *et al.*, 2013). Moreover, the role of several climatic factors has been identified in the seasonal timing and seasonal productivity of vegetation cycles (Ma *et al.*, 2015; Shen *et al.*, 2016). Specifically, in arid and semi-arid environments water availability is deemed to be the primary factor controlling vegetation seasonality and growth (Zhang *et al.*, 2005; Chidumayo, 2015). Of particular interest is the close linkage between precipitation and vegetation growth. Studies have suggested that rainfall control of vegetation greening trends (Hickler *et al.*, 2005; Martínez *et al.*, 2011) was associated with the 1980s recovery of vegetation growth from the Sahelian droughts (Olsson *et al.*, 2005). Likewise, parameters estimated from seasonal growth patterns of vegetated land surfaces have been shown to be correlated with derivatives of rainfall data (Zhang *et al.*, 2005; Guan *et al.*, 2014; Verger *et al.*, 2016). The start of vegetation growing season (SOS) and start of raining season (SRS) have been shown to be highly correlated by several researchers (Zhang *et al.*, 2005; Guan *et al.*, 2014). Despite these general findings, the dynamics of vegetation growth are not identical in areas with similar rainfall regimes, suggesting that rainfall alone does not satisfactorily explain vegetation growth patterns. For example, non-climatic greening was observed in some parts of sub-Saharan Africa (Hoscilo *et al.*, 2014), and no significant relationship was found between SOS and SRS in the northern Sahara desert (Yan *et al.*, 2016).

"Pre-rain green-up" is an interesting phenomenon whereby vegetation growth starts at the end of the dry season, just before the start of the rainy season (Ryan *et al.*, 2017). This phenomenon has been observed as far back as the 1940s in some woody species at the field scale (Miller, 1949). With the emergence of remote sensing of land surface phenology (LSP) (defined as *"the seasonal pattern of variation in vegetated land surfaces observed from remote sensing"* (Friedl *et al.*, 2006)), pre-rain green-up has now been observed across larger

areas, but mostly in African woodlands (Guan *et al.*, 2014; Ryan *et al.*, 2017; Yan *et al.*, 2017). However, the number of studies is limited and does not describe the nature and extent of this relationship at the continental scale. Similarly, only a few studies undertaken at the regional scale have attempted to investigate the lag between the end of rainy season (ERS) and the end of vegetation growing season (EOS) in Africa (Zhang *et al.*, 2005; Yan *et al.*, 2017). Therefore, detailed quantification of the magnitude and frequency of this pattern across different vegetation types at the continental scale is currently needed. Consequently, this research seeks to answer the following questions:

(1) what is the magnitude and spatial distribution of the time lags between vegetation phenophases and rainfall parameters across the different vegetation types in Africa?

(2) what is the magnitude of the association between vegetation phenological and rainfall parameters across the different vegetation types in Africa?

Understanding the relationships between LSP and rainfall parameters is critical in developing a robust phenological model and LSP representation in terrestrial ecosystem models. Currently, most global land-atmosphere models have shown varying projections of vegetation response to climate change, associated with large uncertainties in the terrestrial carbon cycle (Shao *et al.*, 2013). These uncertainties are known to arise from inaccurate estimation of seasonal productivity patterns (Restrepo-Coupe *et al.*, 2017), incorrect assumptions in biosphere–atmosphere process models driven by vegetation growth (Whitley *et al.*, 2016), and poor understanding of functional responses of vegetation phenology to climate change (Richardson *et al.*, 2012). Moreover, current climate change models predict uneven rainfall distribution both in terms of timing and amount across the continent; some areas are expected to receive excess rainfall, whereas other regions are expected to receive less (Res *et al.*, 2001; Niang *et al.*, 2014). This in turn, will affect the vegetation phenology and the resulting vegetation-atmosphere feedbacks such as albedo, water, energy and gas fluxes across the region (Wu *et al.*, 2016).

We used satellite remote sensing and meteorological data to quantify the lag in number of days between SRS and SOS, and ERS and EOS. We further examined the relationships between a range of LSP and rainfall parameters, including the length of growing season (LOS) with length of raining season (LRS), and time of maximum vegetation growth (VItmax) with time of maximum rain (Rtmax), across all of Africa. The productivity-based relationship between Integrated EVI (IntEVI) and cumulative annual rainfall (Rcum) was also explored.

By investigating the above relationships, we provide the most comprehensive and detailed view of the response of vegetation phenological variables to rainfall across Africa, by vegetation type. This greater insight into the mechanisms underlying African vegetation dynamics provides useful information necessary to support and increase the accuracy of future terrestrial biosphere models (TBMs) and global ecosystem models.

Materials and methods

MODIS data and pre-processing

This study used the Moderate Resolution Imaging Spectroradiometer (MODIS) products (Justice *et al.*, 1998) for LSP estimation and land cover classification. These products were downloaded from NASA’s LP DAAC (https://lpdaac.usgs.gov/).

The MODIS/Terra Surface Reflectance 8-Day L3 Global 500 m data (MOD09A1) from February 2000 to June 2016 were selected for LSP estimation. Apart from the delivery of relatively fine spatial detail, the 500 m spatial resolution was selected because it has the spectral bands required to derive the Enhanced Vegetation Index (EVI). These bands are currently absent in finer spatial resolution MODIS data such as the MOD09Q1 and MOD13Q1. The EVI was developed with the inclusion of the blue reflectance band (B) to correct for atmospheric scattering effects and soil background influences (Huete *et al.*, 2011). It is derived according to the following equation:

$$EVI = G * \frac{(NIR - Red)}{(L + NIR + C1 * Red - C2 * Blue)}$$

where the coefficients are L=1 (canopy background adjustment factor); C1= 6 and C2 = 7.5 (aerosol correction factors); and G = 2.5 (gain factor) (Huete *et al.*, 2011).

The EVI was also designed to increase sensitivity in large vegetative biomass regions, consequently overcoming the problems associated with vegetation indices like the normalized difference vegetation index (NDVI) (Huete *et al.*, 2002). Prior to deriving the EVI, residual atmospheric and sensor effects were filtered out and only pixels of the highest quality, which had all possible corrections of MODIS Land Quality Assessment (MODLAND QA), were retained. This was done using the quality assessment procedure as detailed in https://lpdaac.usgs.gov/sites/default/files/public/modis/docs/MODIS_LP_QA_Tutorial-3.pdf ensuring that only high quality pixels were used for this analysis. This involved computing 36 different combinations of MODIS land surface reflectance quality parameters from the 32-bit Science Data Set (SDS) Quality Assurance (QA) layer (the 500 m Reflectance Band Quality). All measurements not within these 36 parameters were filtered out, ensuring that only pixels that were atmospherically and adjacently corrected, and of the highest quality on all bands were retained. To produce a time-series of EVI appropriate to analysing the complex growing seasons in Africa, a “cycle” of approximately two years (i.e., 86 “stacked” layers) of EVI data (i.e., the end of July of year 1 to June of year 3) was used. This long cycle was produced to capture yearly estimates of seasonal phenological parameters across Africa, because start of growing season in the northern latitudes commences much earlier in the year than in the southern latitudes.

To define the vegetation types in Africa, we used the 17-class International Geosphere Biosphere Programme (IGBP) global vegetation classification scheme (Friedl *et al.*, 2002, 2010) from the MODIS/Terra Land Cover Type Yearly L3 Global 500 m data (MCD12Q1). We carried out a reclassification, merging similar classes of plant functional types in the IGBP scheme that differ based on extent of canopy cover only, but have similar phenological behaviour. Table 1 shows the 17 classes and the reclassification applied. Croplands and cropland/natural vegetation mosaic were not merged together because cropland/natural vegetation mosaic is a mixture of croplands, forests, shrublands, and grasslands, which may not be sufficiently well defined for use in modelling the pattern of cropland responses to seasonal rainfall. Homogeneous pixels over the 13 years record of the MCD12Q1 were extracted and used to stratify the land cover into their different vegetation types. Five major classes were derived: (1) Croplands, (2) Forest (Deciduous and evergreen forest), (3) Grasslands, (4) Shrublands (Closed and open shrublands), and (5) Woodlands (Woody savannas and savannas) (see Table 1 and Figure 1). However, due to the limited spatial extent of deciduous forest, and persistent clouds in forested areas, further investigation of the forest category was not considered as estimates of LSP may not be reliable.

CHIRPS data

This study used the 0.05º gridded rainfall dataset from the Climate Hazards Group InfraRed Precipitation with Station data (CHIRPS). This dataset was generated by combining satellite sensor and station data using smart interpolation techniques, and has been shown to have less bias in examining wet seasons than most other products, especially in data-sparse regions in Africa (Funk *et al.*, 2015). It has also been shown to be more precise in estimating the entire seasonal cycle of rainfall because it is spatially more detailed and corresponds more closely to ground data (Toté *et al.*, 2015). As with the MODIS data, 16 years of daily rainfall data from 2000 to 2016 were downloaded from CHIRPS (http://chg.geog.ucsb.edu/data/chirps/).

LSP estimation

Several methods have been used to estimate LSP from time-series of vegetation indices (VI)(Atkinson *et al.*, 2012). These methods usually involve a stepwise approach beginning with the removal of "bad" pixels in the time-series, interpolation of the missing values, smoothing of the complete time-series, and estimation of the LSP parameters. In this research, we used the algorithm from Dash *et al.* (2010) and Pastor-Guzman *et al.* (2018) to remove "bad" pixels and interpolate missing values in the EVI time-series. Then the Discrete Fourier Transform (DFT) (Atkinson *et al.*, 2012) was employed to smooth the data temporally.

The inflection point-based method, which considers points where maximum rate of change occurs in the time-series, was used to estimate the LSP parameters. This method, which has been used extensively, captures explicitly the start and end of growing seasons as there are no pre-defined thresholds (Dash *et al.*, 2010; Qader *et al.*, 2015). A schematic diagram of the methodology is shown in Figure 2. Five LSP parameters (Start of growing season (SOS), End of growing season (EOS), Length of growing season (LOS), time of maximum EVI (VItmax), and Integrated EVI (IntEVI)) were estimated for each cycle (Figure 3). This led to yearly estimates of each LSP parameter for a total of 15 years (2001 – 2015). The derived MODIS Land cover classes were used as a mask to select class-specific LSP parameters.

Estimation of rainfall parameters

The start of rainy season (SRS) and end of rainy season (ERS) have been determined in a variety of ways, and there is still no consensus on the most appropriate definition. Examples can been seen in Liebmann *et al.* (2012) and Yan *et al.* (2016) who employed the climatological anomalous accumulation method in determining the start and end of rainy season, and Zhang *et al.* (2005) and Guan *et al.* (2014) who employed the percentage method. In this research, we adopted the definition first proposed by Stern *et al.* (1981), and used by several researchers and meteorological agencies (Sarria-dodd & Jolliffe, 2001; Segele & Lamb, 2005; Mupangwa *et al.*, 2011). This method defines SRS as the first period of two to 10 days where specified amounts of rainfall (10, 20, 30 mm) are reached or exceeded followed by no continuous dry period of specified length (7, 8, 10 days). This approach was selected as it is designed to also account for sowing dates in croplands to remove false start dates. To determine the wet and dry periods, a threshold was set to differentiate between wet and dry days. All wet days had at least 0.1 mm rainfall and others below this threshold were classed as dry days (Sarria-dodd & Jolliffe, 2001). Two sets of criteria were adopted to determine the SRS: (1) the first wet day in a 40-day duration after a dry spell where the total rainfall in the first consecutive 10 days is 25 mm or more, which is followed by no consecutive dry period of seven days or more, (2) the first wet day in a 30-day duration after a dry spell where the total rainfall in the first consecutive three days in a row is 15 mm or more, which is followed by no consecutive dry period for 10 days or more. If one of the criteria is not met, then testing resumes considering the other. End of season dates were defined as dates after the start of season where no rain occurs over a period of 20 days or, in a 30-day duration, the total number of wet days is less than four (Zhang *et al.*, 2005).

Due to the complexity of rainy seasons in Africa, especially for regions with a bimodal annual rainfall cycle, results were rigorously cross-checked again for false starts. This involved an iterative procedure to check if start dates occurred around 10% accumulation of the total annual precipitation and end dates occurred after 95% accumulation of total annual precipitation. In addition, spatial agreement was seen in the results when compared with previous studies on seasonal rainfall onset and end date retrievals (Zhang *et al.*, 2005; Brown & de Beurs, 2008; Liebmann *et al.*, 2012; Guan *et al.*, 2014). Other rainfall parameters derived were: the length of rainy season (LRS) which is the number of days between SRS and ERS, time of maximum rainfall (Rtmax) and cumulative annual rainfall (Rcum).

Statistical approach

All LSP parameters were aggregated to match the spatial resolution of the rainfall data by assigning the modal value in 10 by 10 0.005^0 grid cells to a 0.05^0 grid cell. The mode was used because the mean can be skewed due to the occurrence of outliers, and the median is less representative of the average of a dataset. Pixels showing no clear vegetation seasonality were excluded from the analysis. Pixels with no distinct rainfall seasonality for the entire time-series were also excluded.

The lag, which is the time difference in number of days between SOS and SRS, and EOS and ERS, was calculated for each land cover type. A -10 and 10 days “no change” category was applied to the start of growing and rainy season lags to account for uncertainties in the SOS and SRS estimates and the MODIS 8-day composites. This range was selected because lags of less than 10 days may sometimes arise due to the difference in the Julian date of the MODIS 8-days composite and the daily rainfall data. Further analysis involved fitting linear regression models to determine the association of spatial shifts with the means of different combinations of LSP and rainfall parameters (Table 2).

Results

Frequency of lags between LSP and rainfall parameters across Africa

The difference between the SRS and SOS can be classified into three categories: SOS arriving (a) before, (b) after, and (c) at the same time as the SRS. Figure 4 presents these differences for cropland, grassland and woodland. Croplands fell mostly in the second category showing SOS arrival after SRS, while grasslands fell into two categories: SOS arriving at the same time as SRS and SOS arriving before SRS. For woodlands, however, SOS arrived much before the SRS.

Across Africa, SOS generally occurred prior to the SRS except in the Sudano-Sahelian region were SOS occurred after the SRS (Figure 5). The distribution of the pixels seen in Figure 5c is skewed towards positive lag values with more occurring between 15 and 45 days (i.e., SOS before SRS). More than 88% of the studied vegetative area had SOS arriving more than 10 days before the SRS, of which 90% was found in woodlands. This phenomenon was distributed across all of Africa, but was ubiquitous in southern Africa, with longer lags concentrated in Angola and Zambia. An estimated 9% of pixels had lags of between -10 and 10 days (i.e. SOS and SRS arriving almost at the same time), with over 90% of these occurring in woodlands. As seen in Figure 5, approximately 3% of the studied vegetation, mainly along the Sudano-Sahelian region, had SOS arriving 10 days or more after the SRS (i.e. < -10 days lag), with over 35% of this area belonging to croplands and about 46% to woodlands. Greater areas of cropland with longer lag times were observed in eastern Africa, particularly in Ethiopia, while woodlands were mostly located in western Africa.

Figure 6 shows the distribution of the lag occurrences within each land cover type. Within cropland, an estimated 10% of pixels had SOS arriving at the same time as the SRS, and over 80% had SOS arriving after the SRS. The average lag times for croplands were -18 days in the north and 54 days in the south. In contrast, over 89% of woodlands had SOS arriving before the SRS, with averages of 29 days in the north and 36 days in the south, with longer lag times in the southern woodlands (Figure 5). Grasslands and shrublands had very similar onset lag patterns, with an early SOS before the SRS in over 80% of pixels with average lags of 38 and 34 days, respectively.

In contrast to the SOS, the EOS generally lagged behind the ERS across all Africa (Figures 4 and 7) with a longer lag duration in southern Africa. Interestingly, the Sudano-Sahelian region also exhibited a distinct lag range of between 90 to 120 days with peaks in western and eastern Africa of 120 to 150 days. In addition, the distribution of pixels (Figure 8c), unlike that for SOS, had several peaks within a wide range of values (50 to 120 days). Over 90% of pixels had a lag of between 30 to 150 days, with the longest durations occurring in woodlands. While most land cover types had varied lags, the lag for over 70% of grasslands varied between 30 to 60 days.

In relation to the season lengths (LOS and LRS), areas with SOS arriving after SRS had shorter LOS (Figure 8), when compared to those with SOS arriving before SRS. The average LOS within these pixels varied between 220±30 days to 250±40 days while those with SOS arriving before SRS varied between 270±45 days to 300±30 days. The LRS within both categories of pixels varied greatly, and no observable pattern was detected.

Spatial relations between LSP and rainfall parameters

Table 2 shows the complex set of spatial associations between LSP and rainfall parameters (all statistically significant at $p < 0.0000$). While a large association was seen between SOS and SRS (R^2= 0.92), IntEVI and Rcum (R^2= 0.58), and VItmax and Rtmax (R^2= 0.52), other combinations of LSP and rainfall parameters showed very little correlation, especially between EOS and ERS, and LOS and LRS. Interestingly, for grasslands, EOS and ERS, and LOS and LRS produced large R^2 values of 0.76 and 0.87, respectively. The same large association was seen across all LSP and rainfall parameters for grasslands. In contrast, only the timings of onset (i.e., SOS and SRS), maxima (i.e., VItmax and Rtmax) and production (IntEVI and Rcum) produced large R^2 values for woodlands. Although, statistically significant, the correlations between EOS and ERS, LOS and LRS, and LOS and Rcum were very small for woodlands. The same association was observed in shrublands between LOS and Rcum. In contrast, a small association was found between SOS and SRS, and between IntEVI and Rcum, in shrublands when compared to all other land cover types.

For croplands, similar to most land cover types (excluding grasslands) the correlation between LOS and LRS was small. In addition, only a small association was observed between VItmax and Rtmax for croplands. However, large correlations were observed for SOS and SRS, and LOS and Rcum.

Discussion

Early and late greening response of vegetation to rainfall

Our results suggest that pre-rain vegetation green-up occurs across most of Africa. The results are corroborated by the pre-rain green-up reported previously by a limited set of studies, both ground-based (Childes, 1989; De Bie *et al.*, 1998; Higgins *et al.*, 2011; Seghieri & Do, 2012; February & Higgins, 2016) and satellite-based (Guan *et al.*, 2014; Ryan *et al.*, 2017; Yan *et al.*, 2017). However, we show that the pre-rain green-up is far more widespread across the entire African continent than previously reported. In addition, we were able to determine quantitatively its occurrence across all the major vegetation types studied, confirming its prevalence mostly in woodlands and grasslands in northern and southern Africa. Our findings show that more pre-rain green-up occurred in woodlands, sometimes as much as 3 months before the onset of rain. This pattern of pre-rain green-up in woodlands was more widespread in the southern part of Africa, consistent with previous work (Ryan *et al.*, 2017).

Several explanations have been proposed for the observed pre-rain green-up. It was suggested that a form of memory mechanism developed from adaptation to previous climatic cues could be responsible for early greening (by about two months) in Miombo woodland in central and southern Africa (Goward & Prince, 1995). Also implicated were daylength and temperature thresholds being responsible for early greening of certain woody plant species in southern Africa (Van Rooyen *et al.*, 1986). Responses of plants to other anticipatory climatic factors besides rainfall have also been reported in the Australian savanna (Prior *et al.*, 2004; Bowman & Prior, 2005). In Senegal, where we also observed pre-rain green-up, it was suggested that air relative humidity occasioned by the Inter-Tropical Convergence Zone (ITCZ) is a major determinant of early leaf flush in this region (Do *et al.*, 2005). Other mechanisms primarily located within plants have been proposed by several researchers. One of these is the rehydration of stem tissues in the dry season caused by reduction in water stress levels following leaf shedding (Reich & Borchert, 1982; Borchert, 1994; Williams *et al.*, 1997). During this rehydration process, when the required water potential for plant cellular development is attained, early leafing begins (Reich & Borchert, 1982). The phreatophytic nature of some woody plants (their ability to tap underground water reserves with deep root systems, and utilize the previous season's water and nutrients) and low water consumption have also been suggested to cause early green up (Roupsard *et al.*, 1999; Guan *et al.*, 2014). Similarly, the ability of some woody plants to withdraw and conserve nitrogen and carbon for later use to construct new leaves from these stored reserves has been implicated in early green up (February & Higgins, 2016). These features give savanna trees competitive advantage over their herbaceous neighbours, which can drive temporal niche separation; a possible explanation for pre-rain green-up (Higgins *et al.*, 2011; February & Higgins, 2016; Ryan *et al.*, 2017). Another interesting phenomenon, which may have influenced the pre-rain green-up observed in western Africa, is the reverse phenology of the widely distributed *Faidherbia albida* (Acacia) tree (Roupsard *et al.*, 1999; Seghieri & Do, 2012). This species enters leaf out during the dry season and sheds leaves during the rainy season. As described above, its unique facultative phreatophytism and low water consumption are responsible for the reversed phenological pattern. Besides climatic or endogenously plant-controlled causes of early greening, biotic factors such as pressures from herbivory have been hypothesised as reasons for early initiation of leafing in some woody plants (Aide, 1988, 1992). It was suggested that this is an antiherbivore defence mechanism by plants, essentially to escape seasonally from herbivores in order to avoid nutrient losses caused by herbivory (Aide, 1992; Rossatto *et al.*, 2009). However, evidence supporting this strategy in Africa savannas is unavailable (Higgins *et al.*, 2011).

Contrary to previous work (Guan *et al.*, 2014), our findings showed pre-rain green-up occurring in the vast majority of grasslands across Africa, albeit with a short duration, mostly within 10 to 30 days. This can be attributed to SOS being triggered by the small bouts of rains that occur just before the actual start of the rainy season. This is possible because grasslands have very high sensitivity to water fluctuations (Scholes & Archer, 1997; Whitecross *et al.*, 2017). In addition, the large R^2 values in Table 2 also suggest this tight coupling of grasslands and water availability across the continent. Our results also showed that pre-rain green-up occurred in some of the shrublands which can be explained by their deep root systems (Childes, 1989).

In contrast to other land cover types, post-rain green-up was largely observed in croplands, all located in the Sudano-Sahelian region (Figures 5 and 6). This region consists mainly of croplands (Figure 1), and is known to have a short rainy season and prolonged dry season (Liebmann *et al.*, 2012; Dunning *et al.*, 2016) (Figure 8). This lengthened dry season usually influences farmers' decision to begin sowing, because despite relying to some extent on climatological history, they generally wait for a major burst of rain and ascertain the status of the soil moisture before commencing sowing (Marteau *et al.*, 2011). The variety of crops being cultivated can also explain the post-rain green-up observed. For example, the different species of millet and sorghum sown are largely dependent on water availability for growth, and these are the main staple crops in the Sudano-Sahelian region, cultivated mostly under rainfed conditions (Guan *et al.*, 2015).

Woodlands and shrublands found in the Sudano-Sahelian region revealed post-rain green-up. Leafing of dominant woody plants in this region is controlled by rainfall and, as mentioned above, this is caused by the occurrence of marked shorter rainy seasons (Seghieri *et al.*, 2009). The woody plants in this region endure long dry seasons of over 8 months. Hence, they depend on the occurrence of the first rains to begin leafing (Seghieri *et al.*, 2009; Seghieri & Do, 2012).

The early and late greening responses of vegetation also influence the lag between ERS and EOS. For example, longer EOS lags were evident in vegetation with pre-rain green-up phenological patterns. According to several researchers, this early greening before the onset of rains enables plants to obtain early access to, and optimally utilize, nutrients released during the first rains; hence, the longer growing season for such plants (Do *et al.*, 2005). Nevertheless, long EOS lag durations were observed in the Sudano-Sahelian region, especially in croplands with post-rain green-up. As mentioned above, the variety of crops affects the phenological pattern. Crops such as cassava, grown mostly in western Africa, are usually harvested 9 to 18 months after sowing (Ezui *et al.*, 2016), thus, leading to long lags between the ERS and EOS.

Relationships between LSP and rainfall parameters

Consistent with previous studies (Zhang *et al.*, 2005; Guan *et al.*, 2014), our analysis revealed large correlations between SOS and SRS across Africa. Notwithstanding this large correlation, vegetation green-up is not driven by rainy season onset as plants green-up early, prior to the rainy season onset. This phenomenon suggests that other factors may have a much greater influence over the onset of the vegetation growing season. However, large correlations were observed for all the major vegetation types in this study, except for shrublands (Table 1), and this is influenced by the spatial variability in SOS dates across Africa (Adole *et al.*, 2018).

The EOS and ERS had a small association for woodlands and croplands, but large association for shrublands and grasslands. This was expected as the EOS for woodlands extends much later than for ERS. Similarly, because the end of the crop growing season depends largely on sowing date and the variety of crops grown (Brown & de Beurs, 2008), only a small correlation between ERS and crop EOS was expected. The tight coupling of grasslands to water explains the large correlation observed for grasslands, and the large associations between all other grassland LSPs and rain parameters analysed in this study (Table 2).

The LOS and the total amount of annual rainfall across Africa produced a large association. However, only a small association was observed for woodlands between LOS and the total amount of annual rainfall, and between LOS and LRS. This suggests that the length and total amount of annual rainfall does not significantly influence the length of growing season for woody vegetation. One reason for this could be the ability of woody plants to minimise transpiration over a long period, especially during dry seasons and at the same time maximise photosynthesis (De Bie *et al.*, 1998), thus, leading to a longer LOS than LRS. Nevertheless, the time of maximum greenness produced a large association with time of maximum rainfall, and seasonal integrated EVI produced a large association with total amount of annual rainfall (Table 2). This suggests that rainfall amount affects the seasonal productivity of woodlands. This is in broad agreement with reported increases in productivity in areas with larger amounts of rainfall in some woody species in South Africa (Shackleton, 1999).
From this research, it is evident that while pre-rain green-up is ubiquitous in Africa, post-rain green-up was limited to the Sudano-Sahelian region. From previous studies (Berg *et al.*, 2011; Marteau *et al.*, 2011) and the results of this research, it can be inferred that the post-rain green-up pattern observed in the Sudano-Sahelian region can be explained by the very short, marked rainy season in the region.

The above observations pose serious challenges for existing terrestrial biosphere models (TBMs) and climate change predictions (Ryan *et al.*, 2017). Currently, TBMs like the dynamic global vegetation models (DVGM) use only precipitation or soil moisture thresholds in modelling the response of dry deciduous plants to climatic factors (Sitch *et al.*, 2008; Zhao *et al.*, 2013). Some examples of phenological models are the meteorological data-based phenology model (Jolly *et al.*, 2005) and the carbon–nitrogen dynamics (CN) model (Wang *et al.*, 2016). They both depend on seasonal water availability as a cue for vegetation phenology in the tropics. This potentially creates a large bias in estimating phenological events because the parametrisation process in these models does not account for the ubiquitous pre-rain greening phenomenon, which may be triggered by other environmental factors.

Another aspect worthy of consideration in these global change models is the feedback role of phenology on climate, mostly through CO_2 uptake (Peñuelas *et al.*, 2009; Wu *et al.*, 2016). As previously mentioned, the African vegetation contributes 38% of the global climate-carbon cycle feedback, mostly coming from its savanna comprised mainly of woodlands (Friedlingstein *et al.*, 2010). In a changing climate of projected increases in temperatures, droughts, soil moisture drying, and decreases in precipitation in Africa, especially southern Africa (Niang *et al.*, 2014), there could be an accompanying shift in precipitation seasonality and intensity. This could result in the delay or absence of the anticipated moisture support for plant growth at the time needed in pre-rain green up woodlands, with likely consequences on net primary productivity. Consequently, this may influence the vegetation-mediated feedbacks on climate systems (a positive feedback on climate change), because of the possible reduction in CO_2 uptake from the African savannas. Similarly, increasing temperatures may influence vegetation-mediated feedbacks on climate change estimates in pre-rain green up plants. Studies have suggested that temperature increases might have caused increased productivity and growth in some southern African woodlands (Bunting *et al.*, 2016; Davis *et al.*, 2017), therefore, potentially leading to greater CO_2 uptake.

In summary, this research presents a comprehensive classification of the different patterns of LSP responses to rainfall in Africa. It confirms the prevalence of pre-rain green-up in Africa, and further demonstrates that this pattern is more widespread across the continent than previously reported. Additionally, we found that both pre-rain and post-rain green-up had a significant influence on EOS lags across different vegetation types. We were also able to quantify the frequencies of these LSP responses (pre-rain and post-rain) across different vegetation types in Africa and provided supporting evidence from previous studies, mostly ground-based. These findings and other advances in phenological studies were possible because of remote sensing methods (Archibald & Scholes, 2007; Studer *et al.*, 2007). As such, the findings are subject to the common limitations associated with these techniques. Examples of limitations are the potential influences from smoothing and LSP estimation techniques, and influences from the type of sensor (Atzberger *et al.*, 2013). Notwithstanding these limitations, the findings and the supporting literature suggest that rainfall is not the only major environmental factor controlling initiation and cessation of vegetation seasonality in Africa. It proposes that although rainfall is important in vegetation growth (as seen in the large correlations between the rainfall and phenological parameters), other environmental factors, and the interplay between these factors, are likely to exert a greater influence on the onset and end of seasonal vegetation growth patterns. Temperature and photoperiodicity have been suggested to be among the most important factors triggering onset of growing season across Africa. The effect of these other factors and the related role of rainfall in seasonal vegetation growth needs to be investigated at the continental scale to advance our understanding of natural ecosystem processes in Africa and their representation in terrestrial biosphere models. This is especially important, considering the need to understand the likely responses of pre-rain green-up under a changing climate, and how these responses might influence global climate change on vegetation-atmosphere feedbacks.

Acknowledgments

The authors would like to thank the Commonwealth Scholarship Commission in the UK for funding and support provided to Tracy Adole. The authors would also like to acknowledge the NASA EOSDIS Land Processes Distributed Active Archive Center (LP DAAC) from which the MODIS data were acquired, the Climate Hazards Group (CHG) for the CHIRPS data, and the anonymous reviewers for their constructive feedback.

References

Adole, T., Dash, J. & Atkinson, P.M. (2016) A systematic review of vegetation phenology in Africa. *Ecological Informatics*, **34**, 117–128.

Adole, T., Dash, J. & Atkinson, P.M. (2018) Characterising the Land Surface Phenology of Africa using 500 m MODIS EVI. *Applied Geography*, **90**, 187–199.

Aide, T.M. (1992) Dry Season Leaf Production: An Escape from Herbivory. *Biotropica*, **24**, 532.

Aide, T.M. (1988) Herbivory as a selective agent on the timing of leaf production in a tropical understory community. *Nature*, **336**, 574–575.

Archibald, S. & Scholes, R.J. (2007) Leaf green-up in a semi-arid African savanna – separating tree and grass responses to environmental cues. *Journal of Vegetation Science*, **18**, 583–594.

Atkinson, P.M., Jeganathan, C., Dash, J. & Atzberger, C. (2012) Inter-comparison of four models for smoothing satellite sensor time-series data to estimate vegetation phenology.

Remote Sensing of Environment, **123**, 400–417.

Atzberger, C., Klisch, A., Mattiuzzi, M. & Vuolo, F. (2013) Phenological Metrics Derived over the European Continent from NDVI3g Data and MODIS Time Series. *Remote Sensing*, **6**, 257–284.

Berg, A., Sultan, B. & de Noblet-Ducoudré, N. (2011) Including tropical croplands in a terrestrial biosphere model: Application to West Africa. *Climatic Change*, **104**, 755–782.

De Bie, S.E., Ketner, P., Paasse, M. & Geerlingt, C. (1998) Woody Plant Phenology in the West Africa Savanna. *Journal of Biogeography*, **25**, 883–900.

Borchert, R. (1994) Soil and stem water storage determine phenology and distribution of tropical dry forest trees. *Ecology*, **75**, 1437–1449.

Bowman, D.M.J.S. & Prior, L.D. (2005) Why do evergreen trees dominate the Australian seasonal tropics? *Australian Journal of Botany*, **53**, 379–399.

Brottem, L., Turner, M.D., Butt, B. & Singh, A. (2014) Biophysical Variability and Pastoral Rights to Resources: West African Transhumance Revisited. *Human Ecology*, **42**, 351–365.

Brown, M.E. & de Beurs, K.M. (2008) Evaluation of multi-sensor semi-arid crop season parameters based on NDVI and rainfall. *Remote Sensing of Environment*, **112**, 2261–2271.

Brown, M.E. & Funk, C.C. (2008) Climate. Food security under climate change. *Science (New York, N.Y.)*, **319**, 580–1.

Buitenwerf, R., Rose, L. & Higgins, S.I. (2015) Three decades of multi-dimensional change in global leaf phenology. *Nature Climate Change*, **5**, 364–368.

Bunting, E.L., Fullman, T., Kiker, G. & Southworth, J. (2016) Utilization of the SAVANNA model to analyze future patterns of vegetation cover in Kruger National Park under changing climate. *Ecological Modelling*, **342**, 147–160.

Chidumayo, E. (2015) Dry season watering alters the significance of climate factors influencing phenology and growth of saplings of savanna woody species in central Zambia, southern Africa. *Austral Ecology*, **40**, 794–805.

Childes, S.L. (1989) Phenology of nine common woody species in semi-arid, deciduous Kalahari Sand vegetation. *Vegetatio*, **79**, 151–163.

Cleland, E.E., Chuine, I., Menzel, A., Mooney, H. a & Schwartz, M.D. (2007) Shifting plant phenology in response to global change. *Trends in ecology & evolution*, **22**, 357–65.

Dash, J., Jeganathan, C. & Atkinson, P.M. (2010) The use of MERIS Terrestrial Chlorophyll Index to study spatio-temporal variation in vegetation phenology over India. *Remote Sensing of Environment*, **114**, 1388–1402.

Davis, C.L., Hoffman, M.T. & Roberts, W. (2017) Long-term trends in vegetation phenology and productivity over Namaqualand using the GIMMS AVHRR NDVI3g data from 1982 to 2011. *South African Journal of Botany*, **111**, 76–85.

Do, F.C., Goudiaby, V.A., Gimenez, O., Diagne, A.L., Diouf, M., Rocheteau, A. & Akpo, L.E. (2005) Environmental influence on canopy phenology in the dry tropics. *Forest Ecology and Management*, **215**, 319–328.

Dunning, C.M., Black, E.C.L. & Allan, R.P. (2016) The onset and cessation of seasonal rainfall over Africa. *Journal of Geophysical Research: Atmospheres*, **121**, 11405–11424.

Ezui, K.S., Franke, A.C., Mando, A., Ahiabor, B.D.K., Tetteh, F.M., Sogbedji, J., Janssen, B.H. & Giller, K.E. (2016) Fertiliser requirements for balanced nutrition of cassava across eight locations in West Africa. *Field Crops Research*, **185**, 69–78.

February, E.C. & Higgins, S.I. (2016) Rapid leaf deployment strategies in a deciduous savanna. *PLoS ONE*, **11**.

Friedl, M.A., McIver, D.K., Hodges, J.C.F., Zhang, X.Y., Muchoney, D., Strahler, A.H., Woodcock, C.E., Gopal, S., Schneider, A., Cooper, A., Baccini, A., Gao, F. & Schaaf, C. (2002) Global land cover mapping from MODIS: Algorithms and early results. *Remote Sensing of Environment*, **83**, 287–302.

Friedl, M.A., Sulla-Menashe, D., Tan, B., Schneider, A., Ramankutty, N., Sibley, A. & Huang, X. (2010) MODIS Collection 5 global land cover: Algorithm refinements and characterization of new datasets. *Remote Sensing of Environment*, **114**, 168–182.

Friedl, M.H., Henebry, G.M., Reed, B.C., Huete, A., White, M. a, Morisette, J., Nemani, R.R., Zhang, X., Myneni, R.B. & Friedl, M. (2006) Land Surface Phenology. *A community white paper requested by NASA*, **April 10**.

Friedlingstein, P., Cadule, P., Piao, S.L., Ciais, P. & Sitch, S. (2010) The African contribution to the global climate-carbon cycle feedback of the 21st century. *Biogeosciences*, **5**, 4847–4866.

Funk, C., Peterson, P., Landsfeld, M., Pedreros, D., Verdin, J., Shukla, S., Husak, G., Rowland, J., Harrison, L., Hoell, A. & Michaelsen, J. (2015) The climate hazards infrared precipitation with stations—a new environmental record for monitoring extremes. *Scientific Data*, **2**, 150066.

Goward, S.N. & Prince, S.D. (1995) Transient Effects of Climate on Vegetation Dynamics: Satellite Observations. *Journal of Biogeography*, **22**, 549.

Grace, J., Jose, J.S., Meir, P., Miranda, H.S. & Montes, R.A. (2006) Productivity and carbon fluxes of tropical savannas. *Journal of Biogeography*, **33**, 387–400.

Guan, K., Sultan, B., Biasutti, M., Baron, C. & Lobell, D.B. (2015) What aspects of future rainfall changes matter for crop yields in West Africa? *Geophysical Research Letters*, **42**, 8001–8010.

Guan, K., Wood, E.F., Medvigy, D., Kimball, J., Ming Pan, K.K.C., Sheffield, J., Xu, X. & Jones, M.O. (2014) Terrestrial hydrological controls on land surface phenology of

African savannas and woodlands. *Journal of Geophysical Research Biogeosciences*, **119**, 1652–1669.

Hemming, D., Betts, R. & Collins, M. (2013) Sensitivity and uncertainty of modelled terrestrial net primary productivity to doubled CO2 and associated climate change for a relatively large perturbed physics ensemble. *Agricultural and Forest Meteorology*, **170**, 79–88.

Hickler, T., Eklundh, L., Seaquist, J.W., Smith, B., Ardö, J., Olsson, L., Sykes, M.T. & Sjöström, M. (2005) Precipitation controls Sahel greening trend. *Geophysical Research Letters*, **32**, 1–4.

Higgins, S.I., Delgado-Cartay, M.D., February, E.C. & Combrink, H.J. (2011) Is there a temporal niche separation in the leaf phenology of savanna trees and grasses? *Journal of Biogeography*, **38**, 2165–2175.

Hoscilo, A., Balzter, H., Bartholomé, E., Boschetti, M., Brivio, P.A., Brink, A., Clerici, M. & Pekel, J.F. (2014) A conceptual model for assessing rainfall and vegetation trends in sub-Saharan Africa from satellite data. *International Journal of Climatology*, n/a-n/a.

Huete, A., Didan, K., Leeuwen, W. Van, Miura, T. & Glenn, E. (2011) *MODIS vegetation indices*. *Land remote sensing and global environmental change* (ed. by B. Ramachandran), C.O. Justice), and M.J. Abrams), pp. 579–602. Springer New York, Springer New York.

Huete, A., Didan, K., Miura, T., Rodriguez, E.., Gao, X. & Ferreira, L.. (2002) Overview of the radiometric and biophysical performance of the MODIS vegetation indices. *Remote Sensing of Environment*, **83**, 195–213.

IPCC (2014) *Climate Change 2014: Impacts, Adaptation, and Vulnerability. Part A: Global and Sectoral Aspects. Contribution of Working Group II to the Fifth Assessment Report of the Intergovernmental Panel on Climate Change*, (ed. by C.B. Field), V.R. Barros), D.J. Dokken), K.J. Mach), M.D. Mastrandrea), T.E. Bilir), M. Chatterjee), K.L. Ebi), Y.O. Estrada), R.C. Genova), B. Girma), E.S. Kissel), A.N. Levy), S. MacCracken), P.R. Mastrandrea), and L.L. White) Cambridge University Press, Cambridge, United Kingdom and New York, NY, USA,1132pp.

Jolly, W.M., Nemani, R. & Running, S.W. (2005) A generalized, bioclimatic index to predict foliar phenology in response to climate. *Global Change Biology*, **11**, 619–632.

Justice, C.O., Vermote, E.F., Townshend, J.R.G., Defries, R.S., Roy, D.P., Hall, D.K., Salomonson, V. V, Privette, J.L., Riggs, G., Strahler, A.H., Lucht, W., Myneni, R.B., Knyazikhin, Y., Running, S.W., Nemani, R.R., Wan, Z., Huete, A.R., van Leeuwen, W., Wolfe, R.E., Giglio, L., Muller, J.P., Lewis, P. & Barnsley, M. (1998) The Moderate Resolution Imaging Spectroradiometer (MODIS): land remote sensing for global change research. *Geoscience and Remote Sensing, IEEE Transactions on*, **36**, 1228–1249.

Keenan, T., Gray, J. & Friedl, M. (2014) Net carbon uptake has increased through warming-induced changes in temperate forest phenology. *Nature Climate Change*, **4**, 598–604.

Liebmann, B., Bladé, I., Kiladis, G.N., Carvalho, L.M. V, Senay, G.B., Allured, D., Leroux, S. & Funk, C. (2012) Seasonality of African precipitation from 1996 to 2009. *Journal of Climate*, **25**, 4304–4322.

Ma, X., Huete, A., Moran, S., Ponce-campos, G. & Eamus, D. (2015) Abrupt shifts in phenology and vegetation productivity under climate extremes. *Journal of Geophysical Research: Biogeosciences*, **120**, 2036–2052.

Marteau, R., Sultan, B., Moron, V., Alhassane, A., Baron, C. & Traoré, S.B. (2011) The onset of the rainy season and farmers' sowing strategy for pearl millet cultivation in Southwest Niger. *Agricultural and Forest Meteorology*, **151**, 1356–1369.

Martínez, B., Gilabert, M. a., García-Haro, F.J., Faye, a. & Meliá, J. (2011) Characterizing land condition variability in Ferlo, Senegal (2001-2009) using multi-temporal 1-km

Apparent Green Cover (AGC) SPOT Vegetation data. *Global and Planetary Change*, **76**, 152–165.

Miller, C.B. (1949) Flowering periodicity in some woody plants of the Southern Bechuanaland Protectorate. *The Journal of South African Botany*, 49–54.

Mupangwa, W., Walker, S. & Twomlow, S. (2011) Start, end and dry spells of the growing season in semi-arid southern Zimbabwe. *Journal of Arid Environments*, **75**, 1097–1104.

Niang, I., Ruppel, O.C., Abdrabo, M.A., Essel, A., Lennard, C., Padgham, J. & Urquhart, P. (2014) *Africa. Climate Change 2014: Impacts, Adaptation, and Vulnerability. Part B: Regional Aspects. Contribution of Working Group II to the Fifth Assessment Report of the Intergovernmental Panel on Climate Change* (ed. by V.R. Barros), C.B. Field), D.J. Dokken), M.D. Mastrandrea), K.J. Mach), T.E. Bilir), M. Chatterjee), K.L. Ebi), Y.O. Estrada), R.C. Genova), B. Girma), E.S. Kissel), A.N. Levy), S. MacCracken), P.R. Mastrandrea), and L.L.White), pp. 1199–1265. Cambridge University Press, Cambridge, United Kingdom and New York, NY, USA.

Olsson, L., Eklundh, L. & Ardö, J. (2005) A recent greening of the Sahel—trends, patterns and potential causes. *Journal of Arid Environments*, **63**, 556–566.

Pastor-Guzman, J., Dash, J. & Atkinson, P.M. (2018) Remote sensing of mangrove forest phenology and its environmental drivers. *Remote Sensing of Environment*, **205**, 71–84.

Peñuelas, J., Rutishauser, T. & Filella, I. (2009) Ecology. Phenology feedbacks on climate change. *Science (New York, N.Y.)*, **324**, 887–888.

Prior, L.D., Bowman, D.M.J.S. & Eamus, D. (2004) Seasonal differences in leaf attributes in Australian tropical tree species: Family and habitat comparisons. *Functional Ecology*, **18**, 707–718.

Qader, S.H., Atkinson, P.M. & Dash, J. (2015) Spatiotemporal variation in the terrestrial vegetation phenology of Iraq and its relation with elevation. *International Journal of*

Applied Earth Observation and Geoinformation, **41**, 107–117.

Reich, P.B. & Borchert, R. (1982) Phenology and ecophysiology of the tropical tree Tabebuia neochrysantha (Bignoniaceae) (Guanacaste, Costa Rica). *Ecology*, **63**, 294–299.

Res, C., Hulme, M., Doherty, R., Ngara, T., New, M. & Lister, D. (2001) African climate change : 1900 – 2100. **17**, 145–168.

Restrepo-Coupe, N., Levine, N.M., Christoffersen, B.O., Albert, L.P., Wu, J., Costa, M.H., Galbraith, D., Imbuzeiro, H., Martins, G., da Araujo, A.C., Malhi, Y.S., Zeng, X., Moorcroft, P. & Saleska, S.R. (2017) Do dynamic global vegetation models capture the seasonality of carbon fluxes in the Amazon basin? A data-model intercomparison. *Global Change Biology*, **23**, 191–208.

Richardson, A.D., Anderson, R.S., Arain, M.A., Barr, A.G., Bohrer, G., Chen, G., Chen, J.M., Ciais, P., Davis, K.J., Desai, A.R., Dietze, M.C., Dragoni, D., Garrity, S.R., Gough, C.M., Grant, R., Hollinger, D.Y., Margolis, H. a., Mccaughey, H., Migliavacca, M., Monson, R.K., Munger, J.W., Poulter, B., Raczka, B.M., Ricciuto, D.M., Sahoo, A.K., Schaefer, K., Tian, H., Vargas, R., Verbeeck, H., Xiao, J. & Xue, Y. (2012) Terrestrial biosphere models need better representation of vegetation phenology: Results from the North American Carbon Program Site Synthesis. *Global Change Biology*, **18**, 566–584.

Richardson, A.D., Keenan, T.F., Migliavacca, M., Ryu, Y., Sonnentag, O. & Toomey, M. (2013) Climate change, phenology, and phenological control of vegetation feedbacks to the climate system. *Agricultural and Forest Meteorology*, **169**, 156–173.

Van Rooyen, M.W., Grobbelaar, N. & Theron, G.K. (1986) Vegetation of the Roodeplaat Dam Nature Reserve. IV. Phenology and climate. *South African Journal of Botany*.

Rossatto, D.R., Hoffmann, W.A. & Franco, A.C. (2009) Differences in growth patterns between co-occurring forest and savanna trees affect the forest-savanna boundary.

Functional Ecology, **23**, 689–698.

Roupsard, O., Ferhi, A., Granier, A., Pallo, F., Depommier, D., Mallet, B., Joly, H.I. & Dreyer, E. (1999) Reverse phenology and dry-season water uptake by Faidherbia albida (Del.) A. Chev. in an agroforestry parkland of Sudanese west Africa. *Functional Ecology*, **13**, 460–472.

Ryan, C.M., Williams, M., Grace, J., Woollen, E. & Lehmann, C.E.R. (2017) Pre-rain green-up is ubiquitous across southern tropical Africa: implications for temporal niche separation and model representation. *New Phytologist*, **213**, 625–633.

Sarria-dodd, D.E. & Jolliffe, I.T. (2001) Early detection of the start of the wet season in semiarid tropical climates of western Africa. *International Journal of Climatology*, **21**, 1251–1262.

Scheiter, S. & Higgins, S.I. (2009) Impacts of climate change on the vegetation of Africa: an adaptive dynamic vegetation modelling approach. *Global Change Biology*, **15**, 2224–2246.

Scholes, R.J. & Archer, S.R. (1997) Tree-Grass interactions in savannas. *Annual Review of Ecology and Systematics*, **28**, 517–44.

Segele, Z.T. & Lamb, P.J. (2005) Characterization and variability of Kiremt rainy season over Ethiopia. *Meteorology and Atmospheric Physics*, **89**, 153–180.

Seghieri, J. & Do, F. (2012) *Phenology of woody species along the climatic gradient in west tropical Africa*. *Phenology and Climate Change* (ed. by X. Zhang), pp. 143–178. IntechOpen, Rijeka, Croatia.

Seghieri, J., Vescovo, A., Padel, K., Soubie, R., Arjounin, M., Boulain, N., de Rosnay, P., Galle, S., Gosset, M., Mouctar, A.H., Peugeot, C. & Timouk, F. (2009) Relationships between climate, soil moisture and phenology of the woody cover in two sites located along the West African latitudinal gradient. *Journal of Hydrology*, **375**, 78–89.

Shackleton, C.M. (1999) Rainfall and topo-edaphic influences on woody community phenology in South African savannas. *Global Ecology and Biogeography*, **8**, 125–136.

Shao, P., Zeng, X., Sakaguchi, K., Monson, R.K. & Zeng, X. (2013) Terrestrial carbon cycle: Climate relations in eight CMIP5 earth system models. *Journal of Climate*, **26**, 8744–8764.

Shen, M., Piao, S., Chen, X., An, S., Fu, Y.H., Wang, S., Cong, N. & Janssens, I.A. (2016) Strong impacts of daily minimum temperature on the green-up date and summer greenness of the Tibetan Plateau. *Global Change Biology*, **22**, 3057–3066.

Sitch, S., Huntingford, C., Gedney, N., Levy, P.E., Lomas, M., Piao, S.L., Betts, R., Ciais, P., Cox, P., Friedlingstein, P., Jones, C.D., Prentice, I.C. & Woodward, F.I. (2008) Evaluation of the terrestrial carbon cycle, future plant geography and climate-carbon cycle feedbacks using five Dynamic Global Vegetation Models (DGVMs). *Global Change Biology*, **14**, 2015–2039.

Skowno, A.L., Thompson, M.W., Hiestermann, J., Ripley, B., West, A.G. & Bond, W.J. (2016) Woodland expansion in South African grassy biomes based on satellite observations (1990-2013): general patterns and potential drivers. *Global Change Biology*, 1–12.

Stern, R.D., Dennett, M.D. & Garbutt, D.J. (1981) The start of the rains in West Africa. *Journal of Climatology*, **1**, 59–68.

Studer, S., Stöckli, R., Appenzeller, C. & Vidale, P.L. (2007) A comparative study of satellite and ground-based phenology. *International Journal of Biometeorology*, **51**, 405–414.

Toté, C., Patricio, D., Boogaard, H., van der Wijngaart, R., Tarnavsky, E. & Funk, C. (2015) Evaluation of Satellite Rainfall Estimates for Drought and Flood Monitoring in Mozambique. *Remote Sensing*, **7**, 1758–1776.

Verger, A., Filella, I., Baret, F. & Peñuelas, J. (2016) Vegetation baseline phenology from kilometric global LAI satellite products. *Remote Sensing of Environment*, **178**, 1–14.

Wang, G., Yu, M., Pal, J.S., Mei, R., Bonan, G.B., Levis, S. & Thornton, P.E. (2016) On the development of a coupled regional climate–vegetation model RCM–CLM–CN–DV and its validation in Tropical Africa. *Climate Dynamics*, **46**, 515–539.

Whitecross, M.A., Witkowski, E.T.F. & Archibald, S. (2017) Savanna tree-grass interactions: A phenological investigation of green-up in relation to water availability over three seasons. *South African Journal of Botany*, **108**, 29–40.

Whitley, R., Beringer, J., Hutley, L.B., Abramowitz, G., De Kauwe, M.G., Duursma, R., Evans, B., Haverd, V., Li, L., Ryu, Y., Smith, B., Wang, Y.P., Williams, M. & Yu, Q. (2016) A model inter-comparison study to examine limiting factors in modelling Australian tropical savannas. *Biogeosciences*, **13**, 3245–3265.

Williams, R.J., Myers, B.A., Müller, W., Duff, G.A. & Eamus, D. (1997) Leaf phenology of woody species in a north Australian tropical savanna. *Ecology*, **78**, 2542–2558.

Wu, M., Schurgers, G., Rummukainen, M., Smith, B., Samuelsson, P., Jansson, C., Siltberg, J. & May, W. (2016) Vegetation-climate feedbacks modulate rainfall patterns in Africa under future climate change. *Earth System Dynamics*, **7**, 627–647.

Yan, D., Zhang, X., Yu, Y. & Guo, W. (2017) Characterizing Land Cover Impacts on the Responses of Land Surface Phenology to the Rainy Season in the Congo Basin. *Remote Sensing 2017, Vol. 9, Page 461*, **9**, 461.

Yan, D., Zhang, X., Yu, Y., Guo, W. & Hanan, N.P. (2016) Characterizing land surface phenology and responses to rainfall in the Sahara desert. *Journal of Geophysical Research G: Biogeosciences*, 2243–2260.

Zhang, X., Friedl, M.A., Schaaf, C.B., Strahler, A.H. & Liu, Z. (2005) Monitoring the response of vegetation phenology to precipitation in Africa by coupling MODIS and TRMM instruments. *Journal of Geophysical Research D: Atmospheres*, **110**, 1–14.

Zhao, M., Peng, C., Xiang, W., Deng, X., Tian, D., Zhou, X., Yu, G., He, H. & Zhao, Z. (2013) Plant phenological modeling and its application in global climate change research: overview and future challenges. *Environmental Reviews*, **21**, 1–14.

Tables

Table 1: Reclassification of land cover types into broad categories based on the International Geosphere Biosphere Programme (IGBP) global vegetation classification scheme.

IGBP number	**Initial land cover types**	**Merged land cover type**
1	Evergreen needleleaf forest	Forest
2	Evergreen broadleaf forest	
3	Deciduous needleleaf forest	
4	Deciduous broadleaf forest	
5	Mixed forest	
6	Closed shrublands	Shrublands
7	Open shrublands	
8	Woody savannas	Woodlands
9	Savannas	
10	Grasslands	Grasslands
12	Croplands	Croplands
14	Croplands/natural vegetation mosaic	Croplands/natural vegetation mosaic
11	Permanent wetlands	Non-vegetative cover
13	Urban and built-up land	
15	Permanent snow and ice	
16	Barren or sparsely vegetated	
17	Water	

Table 2: Correlation between LSP and rainfall across space. The associations are reported in R^2 values all at p-value <0.000.

Pheno-rain combinations	**Correlation (R^2) (p-value<0.000) by land cover class**				
	All	**Croplands**	**Grasslands**	**Shrublands**	**Woodlands**
SOS and SRS	0.92	0.70	0.95	0.31	0.97
EOS and ERS	0.10	0.23	0.76	0.50	0.07
LOS and LRS	0.27	0.18	0.87	0.28	0.09
LOS and Rcum	0.34	0.79	0.82	0.04	0.09
IntEVI and Rcum	0.58	0.37	0.55	0.12	0.57
VItmax and Rtmax	0.52	0.28	0.75	0.72	0.69

Figure captions

Figure 1: Reclassified 2013 MODIS land cover product (MCD12Q1).

Figure 2: Flowchart describing the study methodology in three major steps: (1) data processing, (2) data analysis and (3) statistical analysis.

Figure 3: An illustration of LSP parameters used in this research. Black line illustrates smoothed time-series, (a) Start of season (SOS), (b) End of season (EOS), (c) Length of season (LOS), (d) Time of maximum EVI (VItmax), and (e) Integrated EVI (IntEVI).

Figure 4: Examples of pixel profiles for a complete cycle of EVI and daily rainfall time-series. EVI time-series is represented by green curved lines while rainfall is represented by black bars. Vertical dashed lines show LSP and rainfall parameters (SOS and EOS in green and SRS and ERS in blue). (a) Croplands in the Sudano-Sahelian region showing SOS arriving after SRS, (b) Grasslands in the Sudano-Sahelian region showing SOS and SRS arriving approximately at the same time, (c) Grasslands in southern Africa showing SOS arriving before SRS, and (d) Woodlands in southern Africa showing SOS arriving well before SRS.

Figure 5: Difference in days between SRS and SOS (i.e., SRS - SOS in days). Positive values indicate SOS arriving before SRS while negative values indicate SOS arriving after SRS. (a) Spatial distribution of SOS and SRS difference in number of days. (b) Proportion of pixels by land cover type in different categories of SOS and SRS lag. (c) Frequency distribution of SRS and SOS difference.

Figure 6: Proportion of pixels in each land cover type in the different categories of SOS and SRS lag.

Figure 7: Differences in days between EOS and ERS (i.e., EOS - ERS in days). Positive values indicate EOS arriving after ERS while negative values indicate EOS arriving before ERS. (a) Spatial distribution of EOS and ERS difference in number of days, (b) Proportion of pixels by land cover type in different categories of EOS and ERS lag, (c) Frequency distribution of EOS and ERS difference.

Figure 8: Spatial pattern of the average of LSP and rainfall parameters between 2001 and 2015. (a) SOS and SRS and (b) EOS and ERS (shown in months of the year). (c) LOS and LRS (shown in number of days).

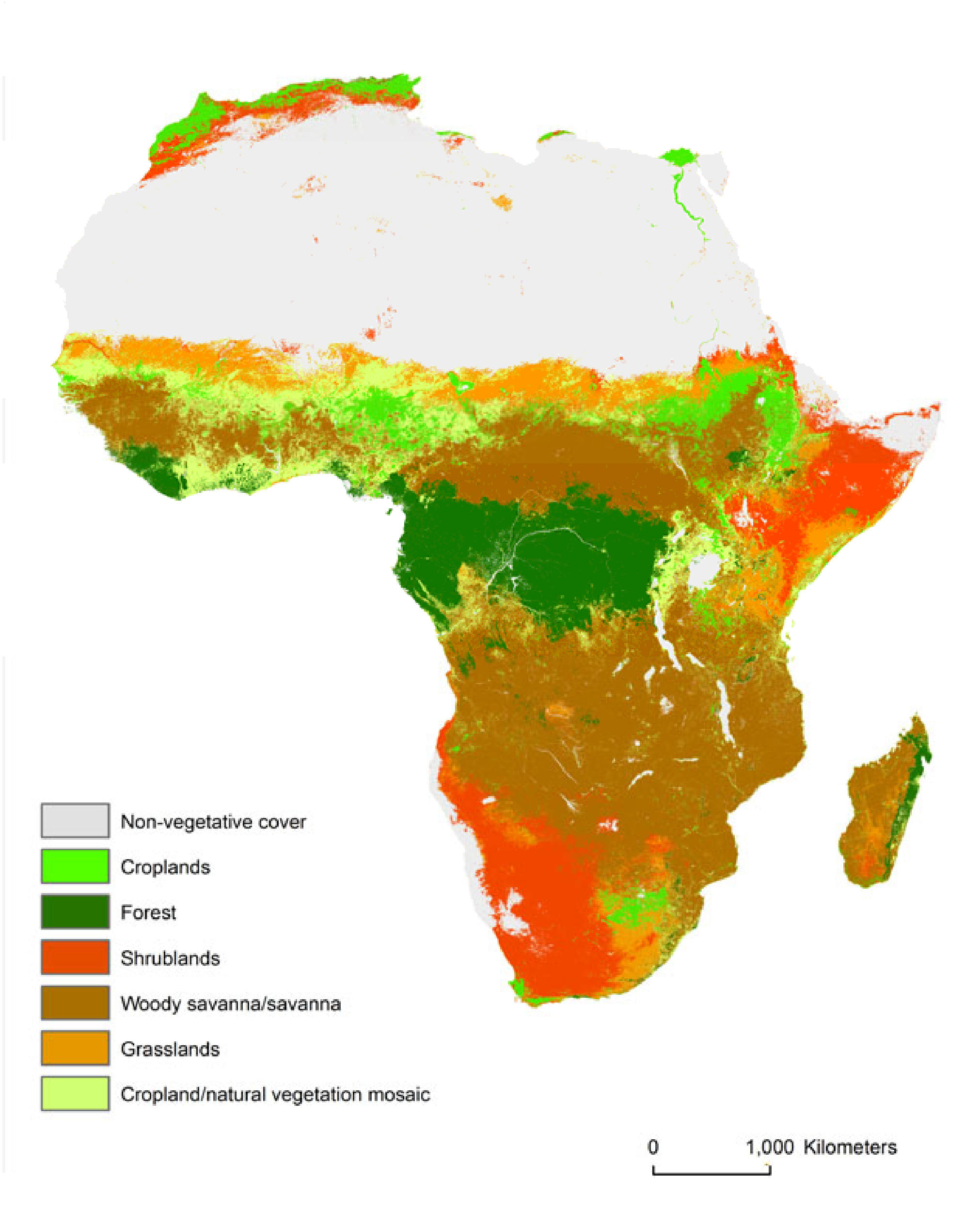
Non-vegetative cover
Croplands
Forest
Shrublands
Woody savanna/savanna
Grasslands
Cropland/natural vegetation mosaic
0
1,000 Kilometers

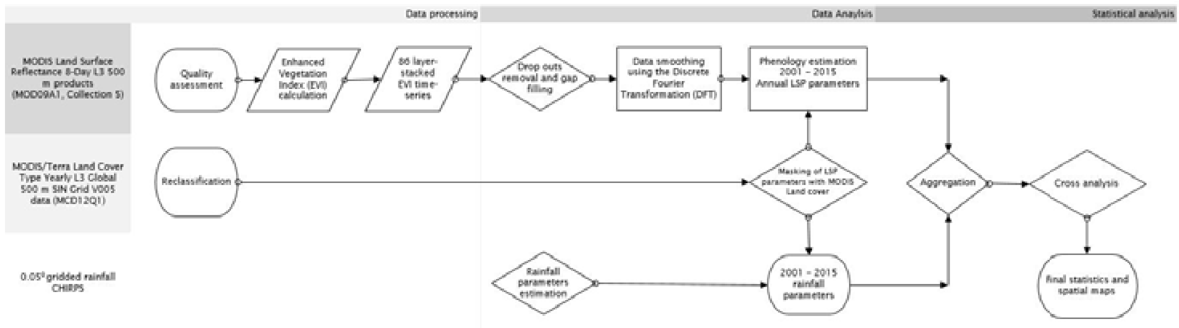
Data processing
Data Anaylsis
Statistical analysis
MODIS Land Surface Reflectance 8-Day L3 500 m products (MOD09A1, Collection 5)
MODIS/Terra Land Cover Type Yearly L3 Global 500 m SIN Grid V005 data (MCD12Q1)
0.05° gridded rainfall CHIRPS
Quality assessment
Enhanced Vegetation Index (EVI) calculation
86 layer-stacked EVI time-series
Drop outs removal and gap filling
Data smoothing using the Discrete Fourier Transformation (DFT)
Phenology estimation 2001 – 2015 Annual LSP parameters
Reclassification
Masking of LSP parameters with MODIS Land cover
Aggregation
Cross analysis
Rainfall parameters estimation
2001 – 2015 rainfall parameters
final statistics and spatial maps

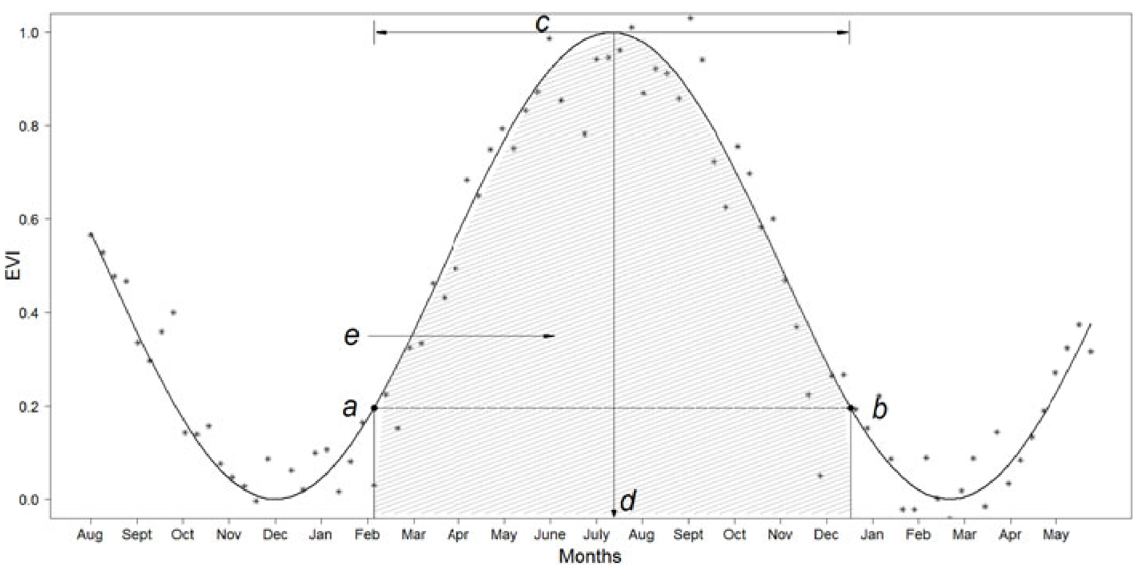
EVI
1.0
0.8
0.6
0.4
0.2
0.0
c
e
a
b
d
Aug
Sept
Oct
Nov
Dec
Jan
Feb
Mar
Apr
May
June
July
Aug
Sept
Oct
Nov
Dec
Jan
Feb
Mar
Apr
May
Months

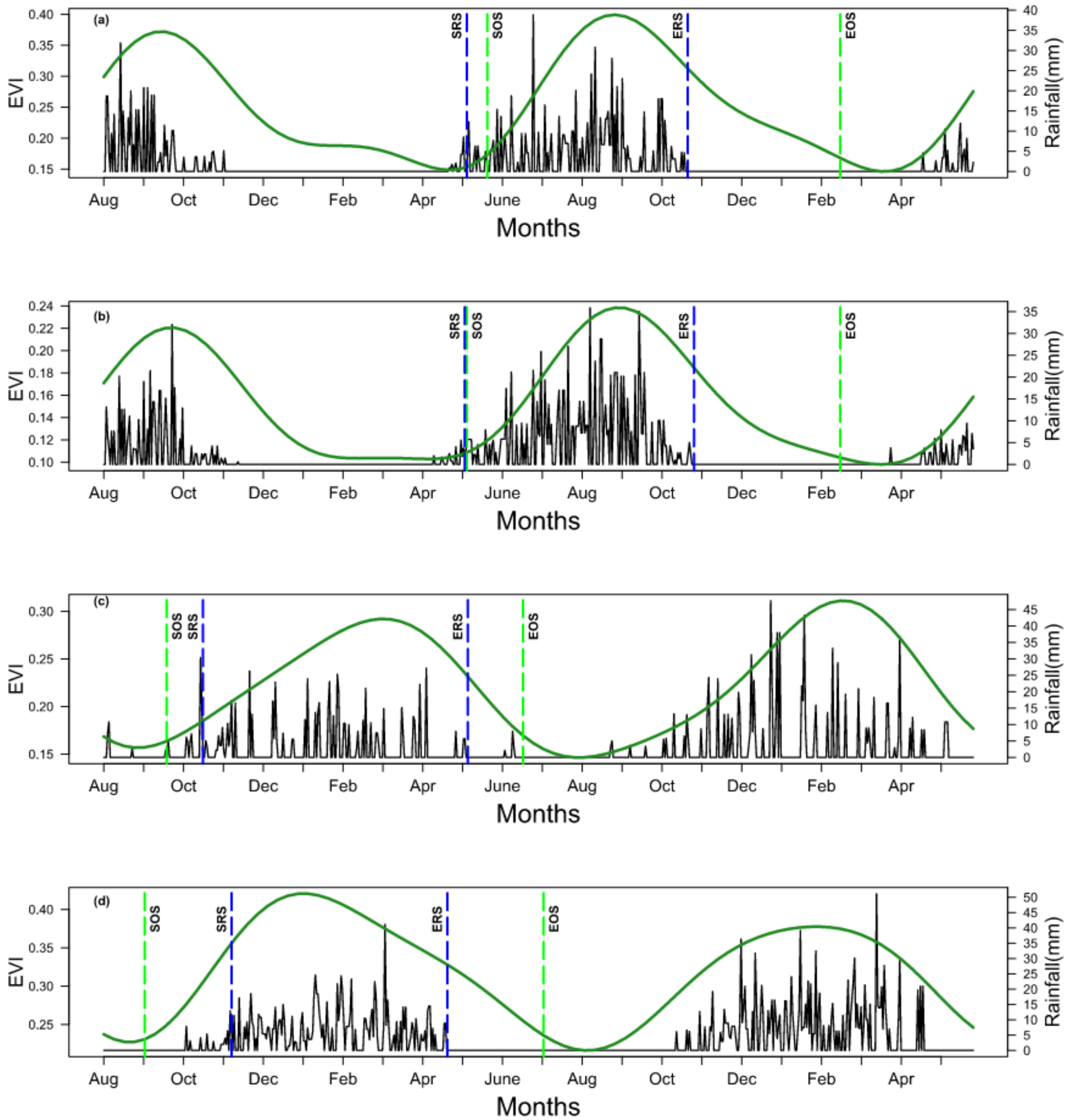
(a)
(b)
(c)
(d)
EVI
Rainfall(mm)
Months
SRS
SOS
ERS
EOS
Aug
Oct
Dec
Feb
Apr
June

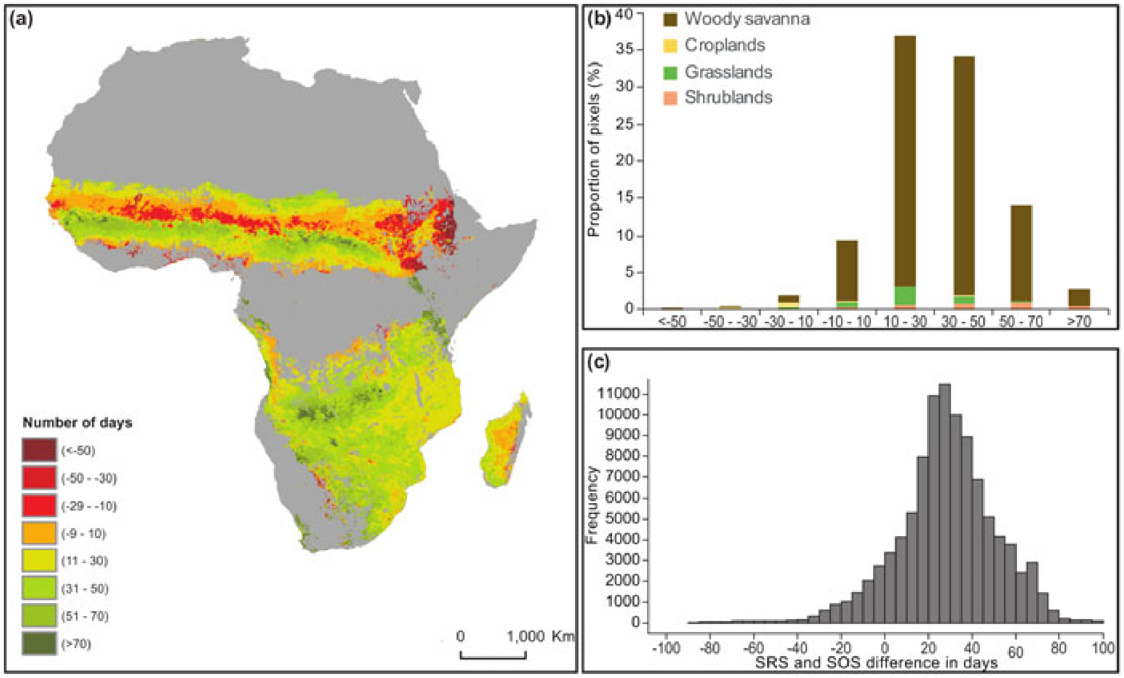
(a)
Number of days
(<-50)
(-50 - -30)
(-29 - -10)
(-9 - 10)
(11 - 30)
(31 - 50)
(51 - 70)
(>70)
0 1,000 Km
(b)
Woody savanna
Croplands
Grasslands
Shrublands
Proportion of pixels (%)
0 5 10 15 20 25 30 35 40
<-50 -50 - -30 -30 - 10 -10 - 10 10 - 30 30 - 50 50 - 70 >70
(c)
Frequency
0 1000 2000 3000 4000 5000 6000 7000 8000 9000 10000 11000
-100 -80 -60 -40 -20 0 20 40 60 80 100
SRS and SOS difference in days

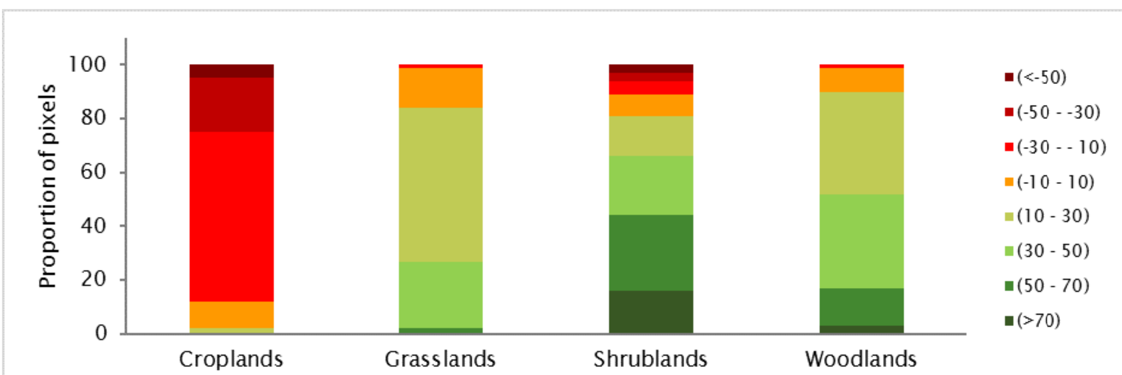
Proportion of pixels
0 20 40 60 80 100
Croplands
Grasslands
Shrublands
Woodlands
(<-50)
(-50 - -30)
(-30 - - 10)
(-10 - 10)
(10 - 30)
(30 - 50)
(50 - 70)
(>70)

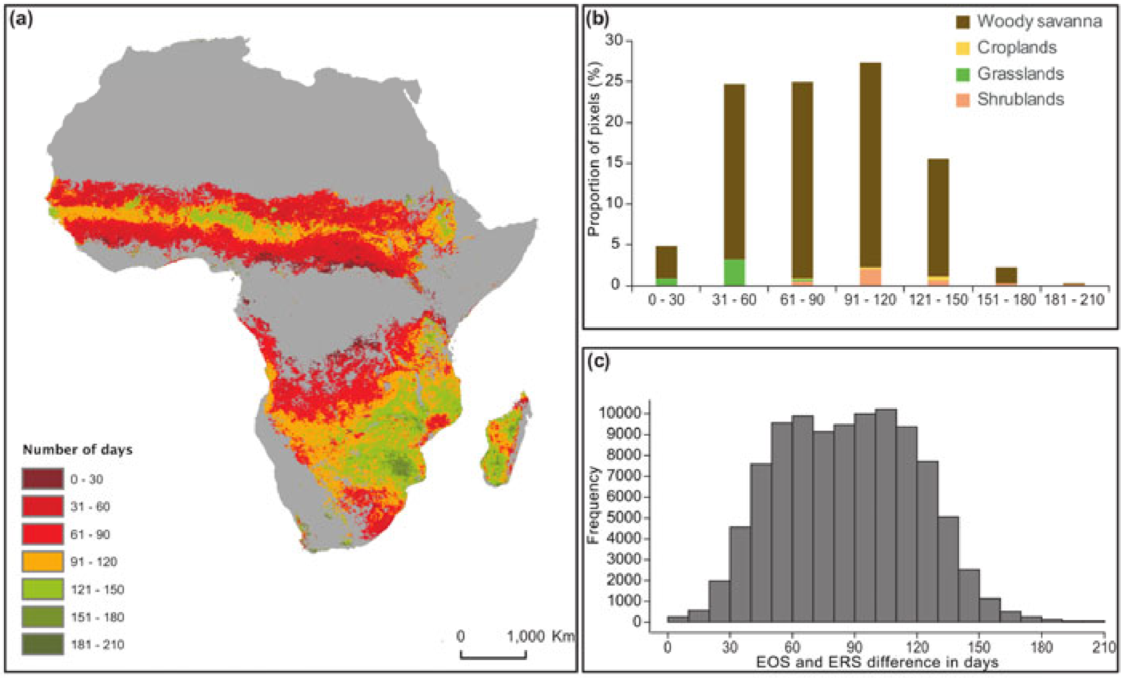
(a)
Number of days
0 - 30
31 - 60
61 - 90
91 - 120
121 - 150
151 - 180
181 - 210
0 1,000 Km
(b)
Woody savanna
Croplands
Grasslands
Shrublands
Proportion of pixels (%)
0 - 30
31 - 60
61 - 90
91 - 120
121 - 150
151 - 180
181 - 210
(c)
Frequency
EOS and ERS difference in days

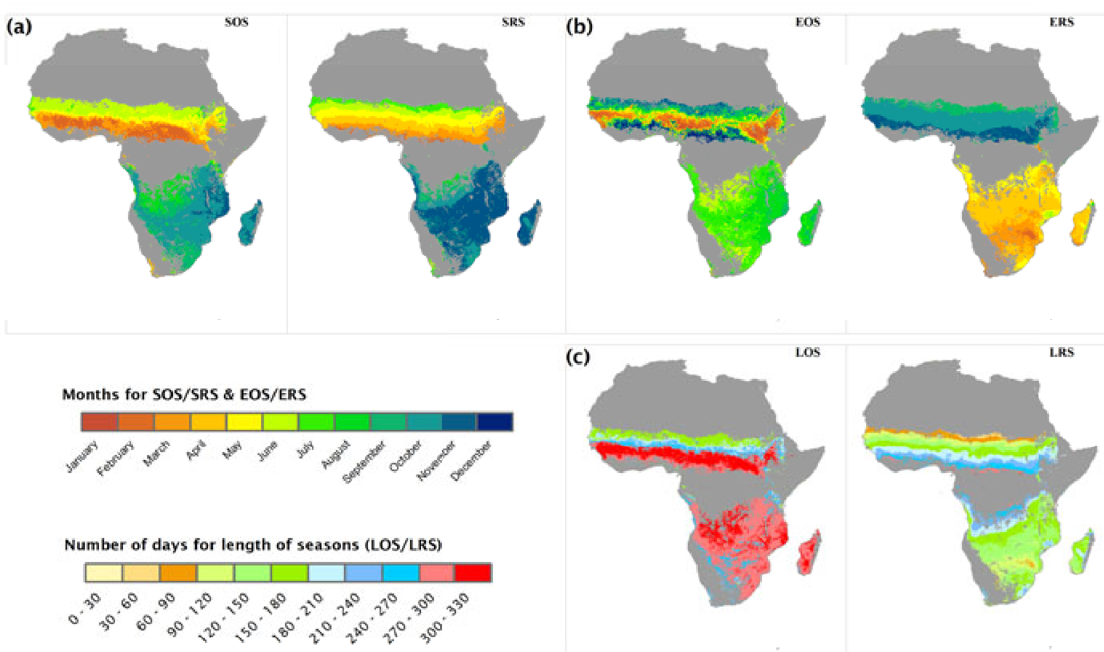
(a)
SOS
SRS
(b)
EOS
ERS
(c)
LOS
LRS
Months for SOS/SRS & EOS/ERS
January
February
March
April
May
June
July
August
September
October
November
December
Number of days for length of seasons (LOS/LRS)
0 - 30
30 - 60
60 - 90
90 - 120
120 - 150
150 - 180
180 - 210
210 - 240
240 - 270
270 - 300
300 - 330